# *Electrochemical Impedance Spectroscopy study of the adsorption of adenine on Au(111) electrodes as a function of the pH*.

F. Prieto*, J. Alvarez-Malmagro, M. Rueda

*Department of Physical Chemistry.University of Seville.C/ Profesor García González nº 1, 41012 Seville (Spain). phone: +34 954557174, e-mail: dapena@us.es*

**ABSTRACT**

The adsorption of the three adenine forms involved in two acid-base equilibria on Au(111) electrodes is studied by Electrochemical Impedance Spectroscopy. The experiments are performed in solutions of pH values 1, 7.5 and 12, at which the cationic, the neutral and the anionic adenine forms are present, respectively. Two adsorption models are adopted, both based on the theory of Frumkin and Melik-Gaykazyan for the adsorption process, but one of them takes also into account a deprotonation step preceding the adsorption step. The same frequency dependence of the impedance data is observed in the three pH media. The Nyquist admittance plots suggest a mixed kinetic control, by adsorption and by diffusion. The analysis of the electrode impedance or admittance as a function of the frequency according to the adsorption models provides the values of adsorption resistance, $R_{ad}$ , adsorption Warburg coefficient, $\sigma_{ad}$ and adsorption capacitance, $C_{ad}$ as a function of potential. From the $\sigma_{ad}$ vs E plot obtained at pH 1 an equilibrium constant for adenine deprotonation at the vicinity of the electrode surface of c.a. 0.03 is calculated, which is three orders of magnitude higher than the equilibrium constant in the bulk solution. The different potential dependency of the adsorption rates at the three pH values is discussed on the basis of a Frumkin isotherm for the adsorption of adenine and a Butler-Volmer type potential dependence for the adsorption rate constant.

## INTRODUCTION

The interaction of biomolecules with well defined solid electrode surfaces is an interesting task because this subject has potential applications in the development of electrochemical biosensors or the design of new nano-platforms for drug delivery. The availability of metallic single crystal electrodes with smooth well oriented surfaces [1], and the biological relevance of DNA derivatives, have prompted us to study the adsorption of DNA bases and derivatives on gold single crystal electrodes.

The adsorption of adenine on low index surfaces of gold single crystal electrodes from neutral solutions was characterised by means of cyclic voltammetry and pseudocapacitance measurements [2]. It was found that the adsorption of adenine strongly depends on the surface orientation and on the reconstructed or unreconstructed state of the electrode. It was concluded that the adsorption of adenine induces the lifting of the reconstruction of the Au(111), as was later confirmed by STM experiments [3]. The experimental capacitance data obtained at potentials within the adsorption/desorption signals showed a clear dispersion with the frequency of the *ac* perturbation that was ascribed to the kinetics of the adsorption process [4].In fact, the smoothness of the single crystal electrode surface, the severe cleaning procedure that assures the absence of any faradaic processes and the specifically designed measurement procedure to avoid interferences by the reconstruction/unreconstruction phenomena permitted the assignment of the frequency dispersion of the capacitance exclusively to kinetics of adenine adsorption and the suitable analysis of the impedance spectra allows us to obtain the characteristic adsorption parameters [4]. In the analysis of the impedance data an adsorption kinetic model was adopted, based on the Frumkin and Melik–Gaykazyan theory [5] that takes into account the mixed kinetic control by transport and by activation of the adsorption [8]. Initially the model assumed a Butler-

Volmer potential dependence of the adsorption rate constant and a Langmuir adsorption isotherm, however the impedance equations that were applied were deduced for a model that avoids any 'a priori' assumption about the dependence of the rate constants of adsorption/desorption with the potential or about the kind of adsorption isotherm [6–9].

The analysis about the kinetics of adenine adsorption by this impedance model was previously limited to solutions of pH values around 7 in which the neutral form of adenine ($AdH_3$) existing in solution can get adsorbed. However, two other adenine forms, the cationic form ($AdH_4^+$) and the anionic form ($AdH_2^-$) can be in solution at other pH values, according to the two protonation/deprotonation equilibria [10,11]:

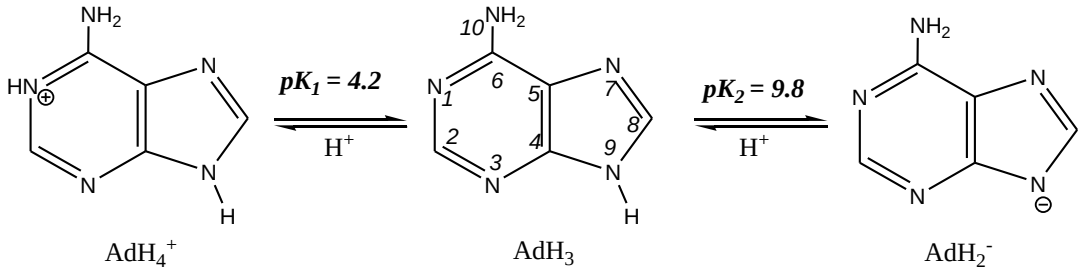


**Scheme 1.-**Acid-base equilibria of adenine in aqueous solutions.

The adsorption of adenine as a function of the pH was studied by cyclic voltammetry and 'in-situ' Fourier transform infrared reflection absorption spectroscopy (FT-IRRAS) [12,13]. It was concluded that from neutral and acid pH solutions, only the neutral adenine is chemically adsorbed, so in very acid solutions where adenine is protonated in solution, the chemical adsorption process of the molecule must include a deprotonation step. On the contrary, at pH values around the second pKa of adenine, both species involved in the equilibrium, the neutral and the anionic adenine forms can be adsorbed, and the pKa value in the interface is very similar to the value in the bulk solution [13].

Recently, we have deduced the impedance equations for an adsorption model based also on the Frumkin and Melik–Gaykazyan model without any "a priori" assumption about the potential dependence of the rate constant for the adsorption or the type of isotherm, but including a deprotonation step preceding the adsorption process [14]. The impedance equations include the equilibrium and the rate constants for the preceding chemical step and predict a frequency dependence different than the one implicit in the previous adsorption kinetic model [6–9,15]

The aim of this article is to take advantage of the possibilities of the impedance analysis to provide kinetic information of adsorption processes on single crystal electrodes in order to explore the differences in the adsorption of the three adenine forms existing in solution at different pH values and to compare their behaviours with the conclusions reached in previous FT-IRRAS studies. With this purpose impedance measurements have been performed at three pH values (pH 1, pH 7.5 and pH 12).

## EXPERIMENTAL

Supporting electrolyte solutions were prepared with highly purified water, freshly obtained from a MilliQ system, and suprapure grade reagents $HClO_4$, NaF and NaOH. Adenine (Sigma-Aldhrich®) working solutions of concentration 1 mM were obtained by the addition of the adequate amount of 10 mM stock solution to the electrochemical cell. All the solutions were degassed by bubbling argon during 20 minutes before running each experiment and then a flow of argon was kept over the solution surface during the measurements.

A three electrode set-up was used for the electrochemical measurements. The working electrode was a Au(111) single crystal, prepared according to the Clavilier method [1]. Before each experiment it was flame annealed with a butane micro-torch and transferred to the electrochemical cell with a water droplet protecting the Au(111) surface from any eventual contamination of the laboratory atmosphere. The contact with the cell solution was made by the meniscus method at a controlled potential low enough as to maintain the reconstructed Au(111) surface obtained with the flame annealing. The counter electrode used was a gold wire also cleaned by flame annealing. The reference electrode was a $Hg/Hg_2SO_{4(s)}/K_2SO_{4(sat)}$ electrode connected to the cell via a salt bridge containing the same supporting electrolyte as in the electrochemical cell.

All the electrochemical measurements were performed with an IviumStat multipurpose electrochemical system, from Ivium Technologies, equipped with a *frequency response analyser*. A single sine ac perturbation with amplitude of 10 mV was applied at frequencies ranging from 20 to 7500 Hz. The adsorption of adenine induces the lifting of the reconstruction of the Au(111) surface obtained during the flame annealing process [2]. Previously to any impedance measurement the Au(111) reconstructed surface was scanned at 10 mV $s^{-1}$ up to a potential higher than the onset of adenine adsorption, $E_{cont}$ , and it was held at that potential during several minutes to guarantee the lifting of the reconstruction of the Au(111) surface. Then, two measurement procedures were assayed: in the *accumulative* procedure the impedance data at a single frequency are obtained as a function of the potential in two consecutive scans in opposite directions, first towards lower potentials and secondly towards higher potential values. This *accumulative* procedure of potential scan permits to check if the electrochemically induced reconstruction of the Au(111) surface at low potentials affects the impedance measurements. In cases where this influence manifests a *step by*

*step* measurement procedure was developed to avoid the interference of the potential induced reconstruction. The procedure was described in [4]. Briefly, it consists in the application of the contact potential (high potential at which adenine is adsorbed) during 60 s before the application of every sample potential, $E_{sample,}$ that is applied during 2 seconds before the impedance measurement. The cycle of potential steps $E_{cont}$ / $E_{sample}$ is repeated for every frequency until the full impedance spectrum has been measured at every sample potential. Following the step by step procedure the impedance spectra are collected at potentials along the adsorption/desorption wave in two series of intercalated potentials, each series with step increment of 40 mV.

## RESULTS AND DISCUSSION

### Pseudocapacitance vs potential plots

In figure 1 the pseudocapacitance, $C_s = (\omega\, Z'')^{-1}$, versus potential plots at 30 Hz, obtained for the adsorption of 1 mM adenine in basic media using the *accumulative* and *step by step* procedures are shown.

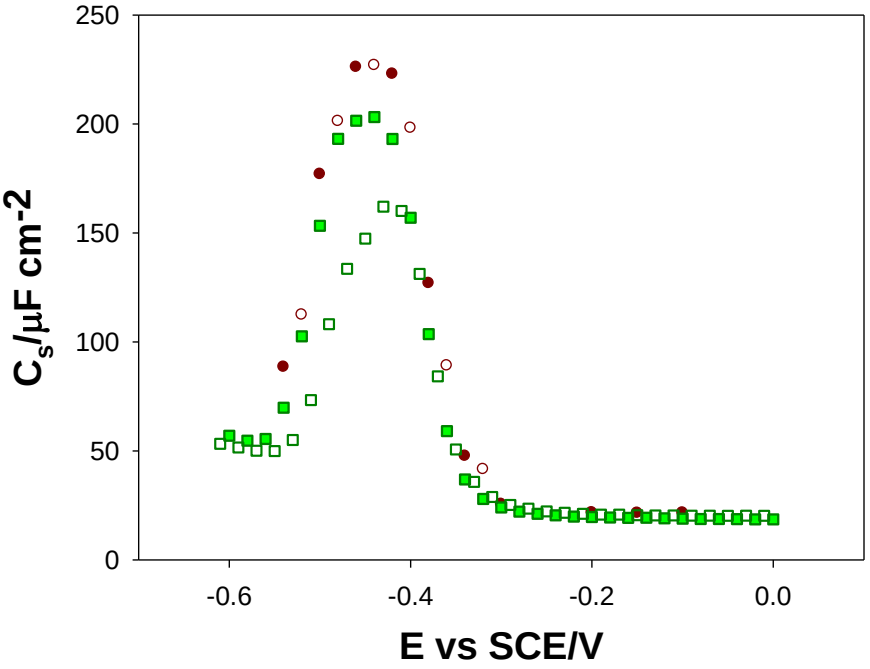


Figure 1.- $C_s$ vs E plots measured at 30 Hz for a Au(111) electrode in contact with 1mM adenine solution in 0.3 M NaF/NaOH of pH 12 with different measurement procedures: *step by step* procedure from -0.1 V to -0.54 V, with $E_{cont}$ = 0V (filled circles) followed by the *step by step* scan from -0.52 to -0.32 V $E_{con\,t}$= 0V (hollow circles); *accumulative* scan from 0 to -0.6 V (filled squares) and subsequent *accumulative* scan from -0.58 to -0.02 V (hollow squares).

The different $C_s$ vs $E$ plots in figure 1 are coincident at potentials higher than c.a. -0.4 V, however clear differences can be observed at lower potentials depending on the measurement procedure. The *step by step* procedure provides an excellent agreement between the two consecutive scans in opposite directions, confirming that the pre-treatment at $E_{cont}$ guarantees the unreconstructed electrode surface before every impedance measurement. However, the $C_s$ values obtained with the *accumulative* procedure clearly deviate from the plot obtained with the *step by step procedure* at

potentials around the maximum of the plot and show clear hysteresis between the negative and the positive scans. It suggests that the electrochemical reconstruction taking place while scanning the low potential region is affecting the measurement. Therefore, all the results shown below have been measured by the *step by step* procedure.

The influence of pH in the pseudocapacitance vs potential plots at two frequencies values (30 and 938 Hz) for adenine adsorption is shown in figure 2 for 1mM adenine concentration in solution. It can be observed that the maximum of the capacitance plots shifts from c.a. -0.02 V to -0.38 V when the pH changes from 1 to 7.5, but with similar values around 120-150 μF cm$^{-2}$ at 30 Hz. At pH 12 the $C_s$ maximum shifts only 0.06 V, up to -0.44 V, however the value is nearly twofold the values obtained at pH 1 and pH 7.5.

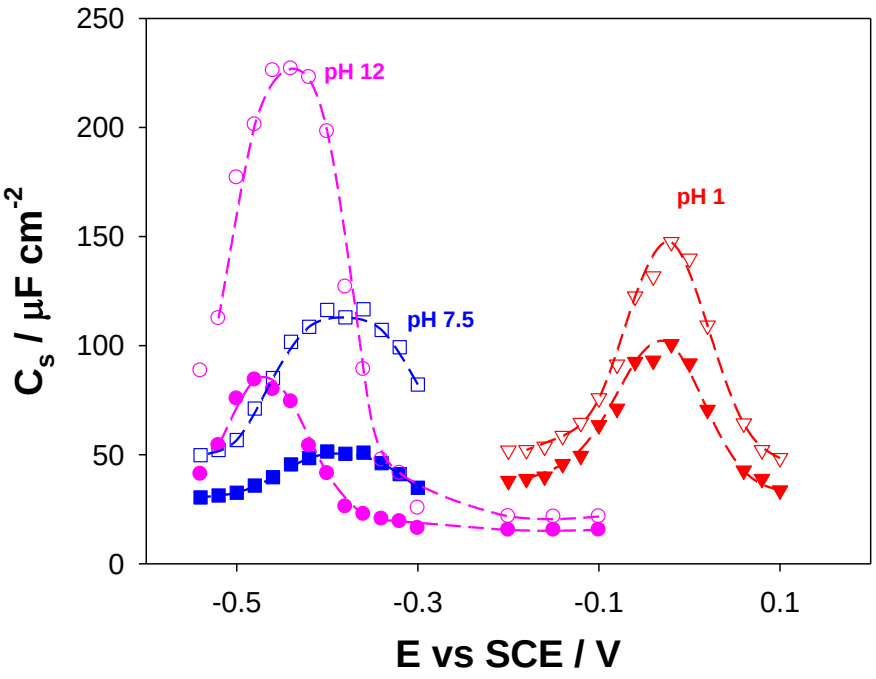


Figure 2.- $C_s$ vs E plots obtained at 30 Hz (hollow symbols) and at 998 Hz (filled symbols) with the *step by step* procedure in two series of alternating potentials for the adsorption of adenine 1 mM on Au(111) electrodes from solutions of pH=1 (triangles), pH=7.5 (squares) and pH=12 (circles).

Fig 2 also shows the influence of the frequency on the pseudocapacitance.

There is a clear dependence of $C_s$ with the frequency at potentials around the maximum. As the frequency increases the peak decreases and slightly shifts towards lower potentials. However, at potential values higher than the onset of adenine adsorption, the dependence of $C_s$ with frequency is negligible.

In the study of adsorption processes on solid electrodes the deviations from a series RC circuit are usually analysed by a constant phase element (CPE) which have an impedance $Z_{CPE} = (Q\ i\ \omega)^{-\alpha}$ with $Q$ and $\alpha$ (ranging from 0 to 1) being frequency independent parameters. For an ideal RC behaviour the CPE parameter $\alpha$ =1. A CPE is sometimes ascribed to surface roughness, heterogeneities or faradaic processes due to impurities.

In this paper the CPE analysis has been applied to quantify the deviation from a series RC (implicit in the frequency dispersion of the pseudocapacitance curves showed in figure 2) to illustrate the correlation of the CPE parameters with the kinetics of adenine adsorption. In figure 3 the values of $\alpha$ obtained at different pH are plotted versus the potential. It can be observed that $\alpha$ clearly deviates from 1 at potentials within the capacitance peak at each pH. The lowest values are obtained at pH 12.

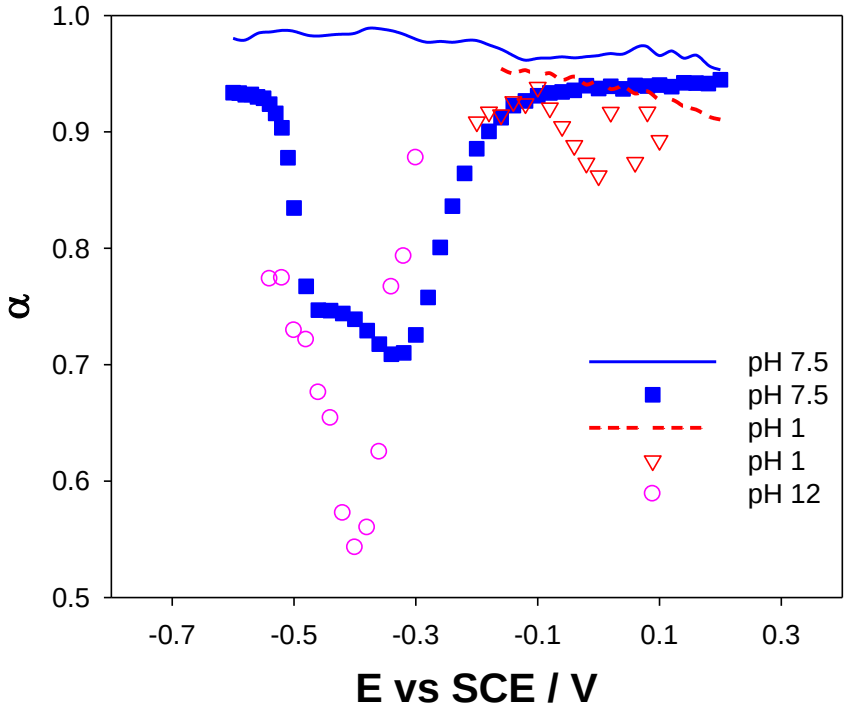


Figure 3.- Plots of the CPE parameter $\alpha$ vs E for adenine adsorption from 1 mM solutions (symbols) at the indicated pH. The results for the supporting electrolyte (lines) are included for comparison.

On the contrary, at potentials far from the corresponding capacitance peaks or at any potential in the absence of adenine, the values obtained for $\alpha$ are close to 1, so the frequency dispersion in these conditions can be neglected. Only the $\alpha$ values obtained in the absence of adenine in acid media are somewhat lower (around 0.9) at potentials of adenine adsorption, probably due to the specific adsorption of the supporting electrolyte anions at the high potentials at which adenine adsorption takes place in acid media, but still the differences with the $\alpha$ values in the presence of adenine are significant.These facts and the smoothness of the Au(111) electrode surface permits to discard that the frequency dispersion is caused by surface roughness or heterogeneities. The *step by step* measurement procedure avoid the interference of surface reconstruction/removal of reconstruction phenomena. Moreover due to the strict cleaning conditions no faradaic process takes place in the experimental conditions. Therefore, the capacitance

dispersion with the frequency must be ascribed to kinetic effects of the adenine adsorption process, so the impedance data for adenine adsorption have been analysed in accordance with the corresponding adsorption kinetics model.

**Analysis with the frequency.**

As mentioned above, in a previous work [4] the impedance spectra obtained for the adenine adsorption on Au(111) electrodes from neutral solution were analysed with the Frumkin and Melik-Gaykazyan kinetic model [5]. In this model the net adsorption rate is defined as:

$$v = \frac{d\,\Gamma}{dt} = k_{ad}\, f_{ad}(\Gamma)\, c_{x=0} \;-\; k_d\, f_d(\Gamma) \qquad (1)$$

Where $k_{ad}$ and $k_d$ are the potential dependent rate constant of the adsorption and desorption steps respectively, $f_{ad}(\Gamma)$ and $f_d(\Gamma)$ are monotonic functions of the surface excess, $\Gamma$, that depend on the adsorption isotherm and $c_{x=0}$ is the adsorbate concentration in the supporting electrolyte at zero distance from the electrode. Sluyters-Rehbach [15] and Kerner and Pajkossy [8] deduced the expression for the adsorption impedance corresponding to this model for semi-infinity diffusion, $Z_{ad}$:

$$Z_{ad} = R_{ad} + \frac{\sigma_{ad}}{(i\,\omega)^{1/2}} + \frac{1}{C_{ad}\, i\,\omega} \qquad (2)$$

Equation (2) includes three frequency independent parameters: the adsorption resistance, $R_{ad}$, the adsorption Warburg coefficient, $\sigma_{ad}$, and the adsorption capacitance $C_{ad}$. $\omega$ is the angular frequency of the ac signal and $i$ is the complex unit.

The impedance of the electrochemical cell must also account for the double layer charge impedance, characterised by a capacitance $C_{dl,\Gamma}$ in a parallel branch to the adsorption

process, and the electrolyte solution ohmic resistance $R_s$ in a series branch. Therefore, the electrochemical cell can be represented by the equivalent circuit in scheme 2.

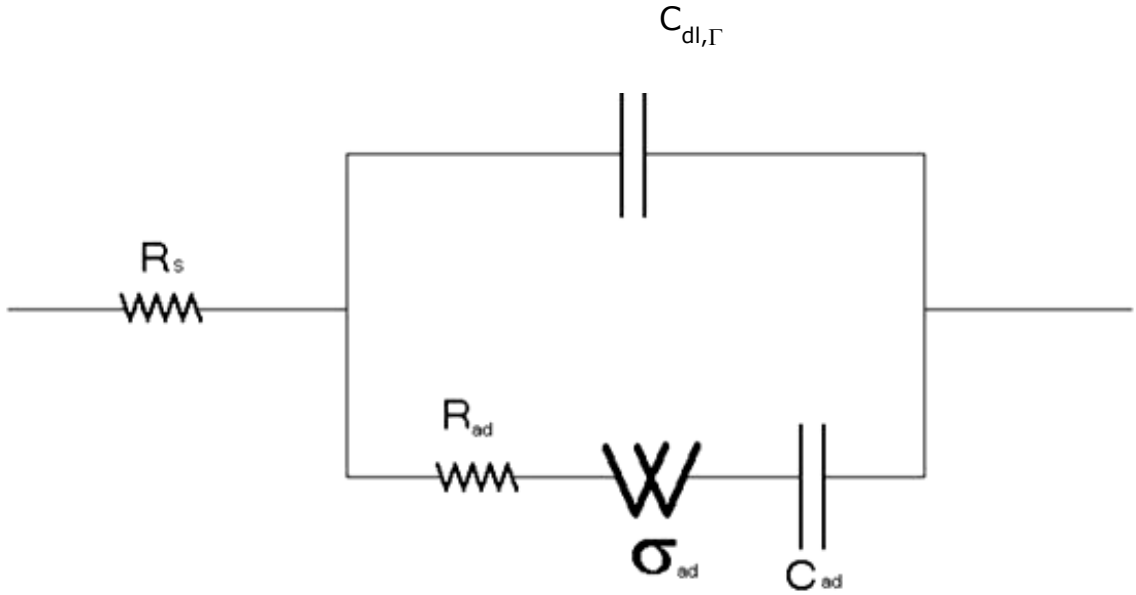


**Scheme 2.-** Equivalent circuit of the electrochemical cell according to the adsorption kinetic model developed in [8,15].

The impedance of the electrochemical cell corresponding to the circuit in scheme 2, is given by:

$$Z_{cell} = R_s + \left[ C_{dl,\Gamma}\, i\, \omega + \left( R_{ad} + \frac{\sigma_{ad}}{(i\, \omega)^{1/2}} + \frac{1}{C_{ad}\, i\, \omega} \right)^{-1} \right]^{-1} \qquad (3)$$

According to this equation, the extrapolation of the real component of the cell impedance to high frequencies provides the ohmic resistance. However, in order to obtain the adsorption parameters the experimental data are better analysed using the interfacial admittance, $Y_{el}$ , that is the inverse of the electrode impedance (obtained from the experimental cell impedance once the ohmic resistance has been subtracted).

$$Y_{el} = \frac{1}{Z_{cell} - R_s} = C_{dl,\Gamma}\, i\,\omega + \left[R_{ad} + \sigma_{ad}(i\,\omega)^{-1/2} + (C_{ad}\, i\,\omega)^{-1}\right]^{-1} \qquad (4)$$

According to this equation, the Nyquist plot (or complex frequency normalised admittance plots) of $Y'_{el}/_{\omega}$ vs $Y''_{el}/_{\omega}$ , with $Y'_{el}$ and $Y''_{el}$ being the real and imaginary components of the electrode admittance, can provide a global view about the nature of the kinetic control of the adsorption process: for a pure kinetic control by activation of the adsorption, a perfect semicircle arc, with the centre in the abscises axis will appear. For a pure kinetic control by diffusion the semicircle arc has the centre below the abscises axis, forming a "depressed" semicircle arc. For a mixed control by adsorption activation and diffusion, a deformed arc is obtained [4,8,15].

Figure 4 shows some representative complex frequency normalised admittance plots at three different pHs for the adsorption of adenine on Au(111) electrodes.

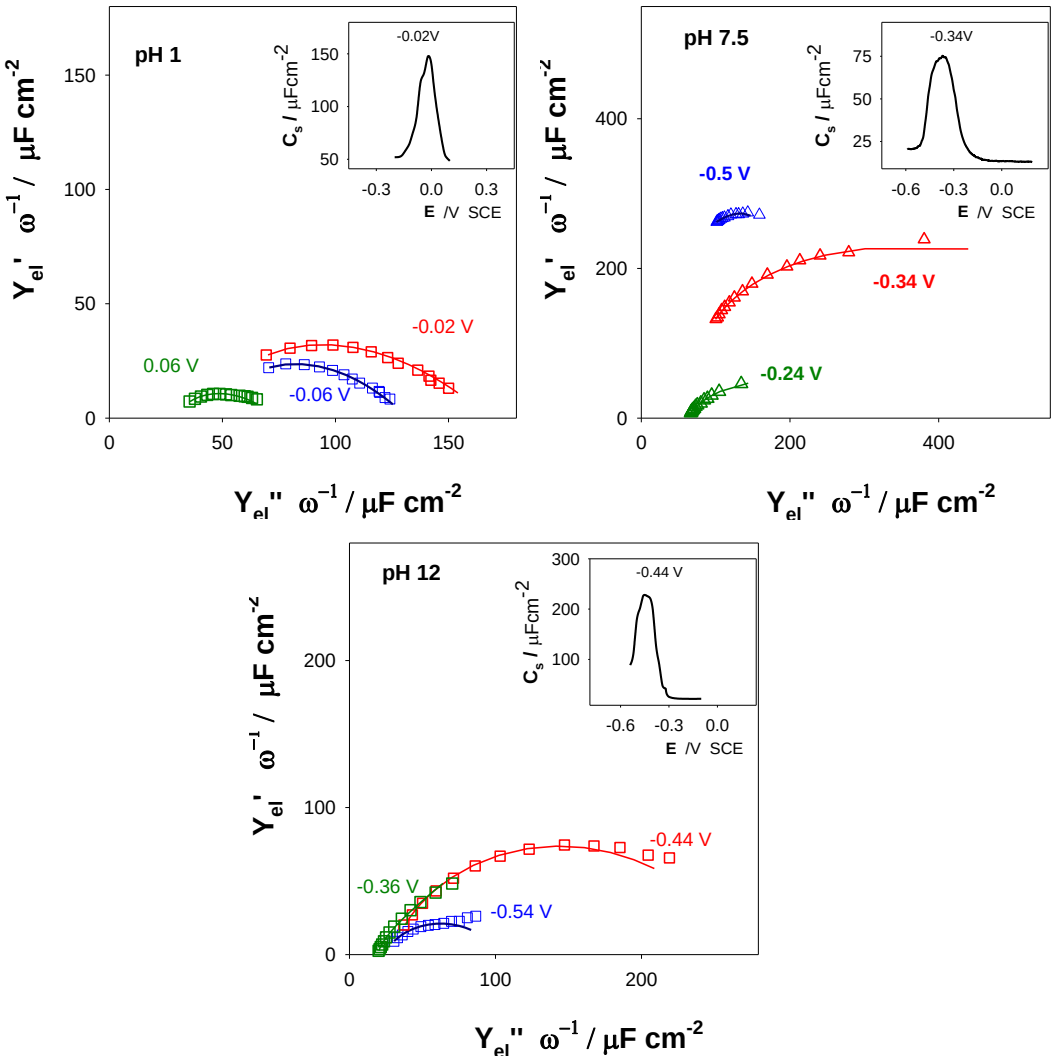


Figure 4.-Nyquist frequency normalised admittance plots for the adsorption of adenine on Au(111) electrodes from 1 mM solutions at the pH and potential values indicated in the plots. The insets at each pH correspond to the pseudo-capacitance vs potential plot obtained in the same conditions at 30 Hz. The solid lines correspond to the theoretical plots calculated with the parameters obtained from the analysis with the frequency.

The plots in figure 4 are depressed semicircle arcs, although partially deformed. This suggests the preponderance of kinetic control by diffusion instead of kinetic control by adsorption activation. The length of the arcs for the same frequency range increases as the potential of the spectrum is closer to the capacitance peak.

The analysis with the frequency of the experimental admittance data according to equation (4) will provide the values of the four frequency independent parameters $C_{dl,\Gamma}, R_{ad}$, $\sigma_{ad}$ and $C_{ad}$ . One of the advantages of using the electrode admittance

instead of the electrode impedance is that the real component of the electrode admittance does not depend on the $C_{dl,\Gamma}$ parameters, so the experimental data can be fitted to the theoretical equation using only three adjustable parameters. Recently we have shown that the frequency dependence of the real component function $Y'_{el}/\omega$ is to be preferred for the fitting as the $Y'_{el}/\omega$ vs $\omega^{1/2}$ plots can show characteristic peaks which in the case of an adsorption system with a preceding chemical step are very sensitive to the equilibrium and rate constants of the chemical step, [14]. Moreover, the corresponding imaginary function $Y''_{el}/\omega$ provides the value of $C_{dl,\Gamma}$ by extrapolation at high frequencies and the value of $C_{dl,\Gamma} + C_{ad}$ at the lowest frequencies. Therefore, the combination of both frequency limits provides a good initial value for $C_{ad}$ to be used in the fitting of the real component function, so that the three adsorption parameters $R_{ad}$, $\sigma_{ad}$ and $C_{ad}$ can be usually obtained with precision from the fitting of the $Y'_{el}/\omega$ vs $\omega^{-1/2}$ plots to the theoretical corresponding equation. The values of these three parameters so obtained are used as starting values for the fitting of the imaginary function $Y''_{el}/\omega$ vs $\omega^{-1/2}$ to the corresponding theoretical equation in order to obtain also the $C_{dl,\Gamma}$ parameter in addition to the other three parameters. The differences between the values of the three parameters that are obtained from the fitting to the real and to the imaginary functions are within the standard deviations with which each parameter is obtained. Moreover, the simultaneous four adjustable parameters analysis to both components of the electrode admittance using as initial estimates the values previously obtained in the separate analysis to each component provides an excellent agreement between the experimental and generated curves and consistent parameters

values, which have been plotted in figure 6. The qualities of the fittings are shown in figure 5 for the adsorption at the three pH values studied at potentials close to their respective pseudocapacitance maximums. An excellent agreement is found between the experimental values and the generated curves (represented by continues lines in Fig. 5) using the theoretical equations and the parameters obtained from the analysis.

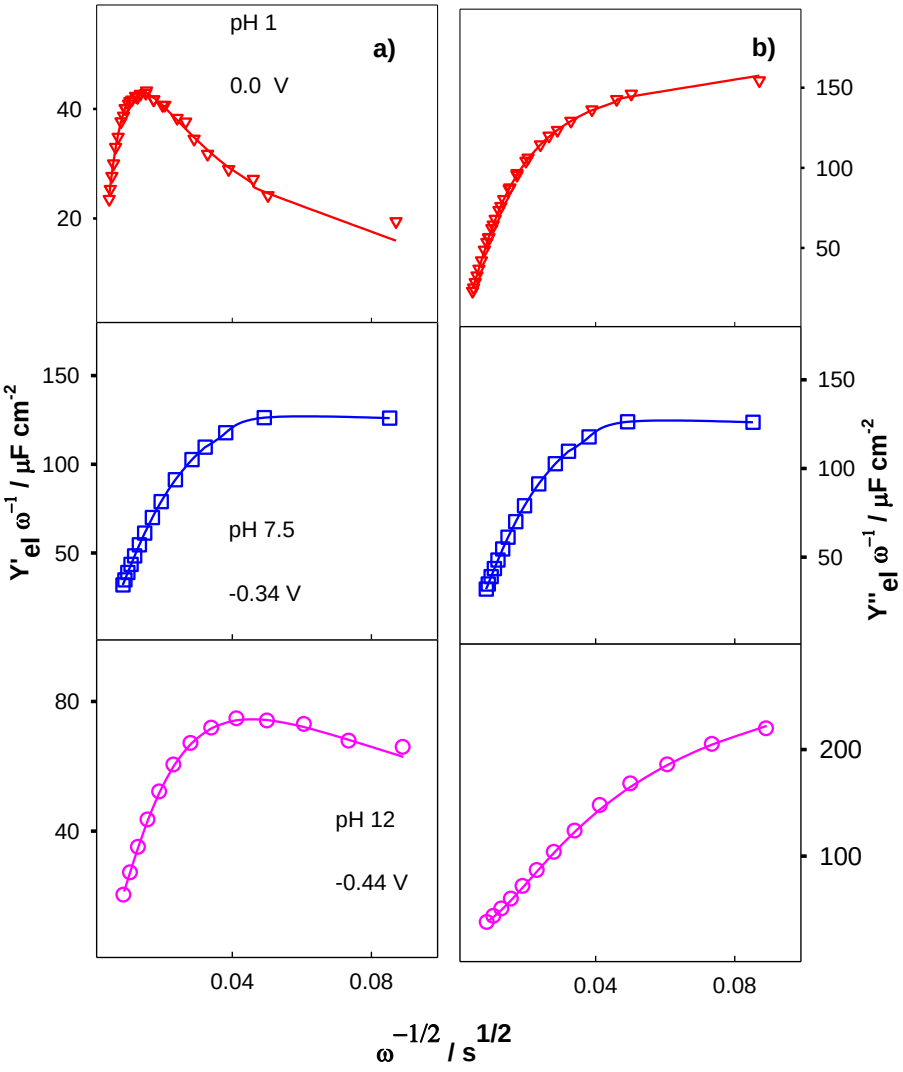


Figure 5.- Plots of $(Y'_{el}\ \omega^{-1})\ vs\ \omega^{-1/2}$ (a) and $(Y''_{el}\ \omega^{-1})\ vs\ \omega^{-1/2}$(b) at the indicated pH and potential values. The symbols represent the experimental plots and the lines the theoretical ones generated with the parameters obtained from the analysis with the frequency.

It is specially remarkable that the admittance data at pH 1 fit the equations corresponding to the circuit in scheme 2, although the general impedance or admittance

equations for a model including a deprotonation reaction preceding the adsorption step do not provide the same frequency dispersion [14]. However, the pronounced peak observed in the $Y'_{el}/_{\omega}$ vs $\omega^{-1/2}$ plot for the results at pH 1 suggests the existence of the chemical coupled reaction, [14].

Effectively, in the case of the model including a chemical step preceding the adsorption step the impedance should account also for the rate of the deprotonation step, previous to the adsorption one, that can be expressed by:

$$v_{chem} = \frac{d\, c_{AdH_3}}{dt} = k_1 c_{AdH_4{}^+} \; - \; k_{-1} c_{AdH_3} c_{H^+} \qquad (5)$$

$k_1$ and $k_{-1}$ are the forward and backward rate constants of the chemical step, respectively. For the second step the same definition of net rate in equation (1), with $c \;\; = c_{AdH_3}$ is still valid.

The equation for the adsorption impedance according to this kinetic model with coupled chemistry has been derived [14], assuming that the mass transport under the ac perturbation is exerted by semi-infinite linear diffusion (with equal diffusion coefficient for the cationic and the neutral adenine molecules) and by the preceding chemical reaction:

$$Z_{ad} = R_{ad} + \sigma_{ad}\left[\frac{K'_1}{K'_1 + 1}(i\,\omega)^{-1/2} + \frac{1}{K'_1 + 1}(k \;\; + i\,\omega)^{-1/2}\right] + \frac{1}{C_{ad}\, i\,\omega} \qquad (6)$$

Where $K'_1 = k_1/_{k'_{-1}}$ is the apparent equilibrium constant, with $k'_{-1} = k_{-1} c_{H^+}$ and $k = k_1 + k'_{-1}$ . It must be noted here that the backwards chemical step has been considered a pseudo-first order process, as the concentration of $H^+$ ions is much higher than the adenine concentration, at the experimental conditions at which the model is

planned to be applied (pH 1). The frequency dependence of the impedance cell according to equation (6) is different from the dependence expressed in equation (3) for an adsorption process without coupled chemistry. However, two limiting cases can be distinguished (depending on the relative values of the chemical step rate constant and the range of frequencies used in the measurements) for which the frequency dependence is the same as implicit in equation (3).

In the *low frequency limit*, that applies if $k \gg \omega$, the general equation (6) can be simplified to:

$$(Z_{ad})^{LF} = R_{ad} + \sigma_{ad}\,\frac{k^{-1/2}}{K_1' + 1} + \sigma_{ad}\,\frac{K_1'}{K_1' + 1}\,(i\,\omega)^{-1/2} + (C_{ad}\,i\,\omega)^{-1} \qquad (7)$$

Equation (7) involves the same frequency dependence of the impedance cell expressed in equation (3) but with a different meaning for the apparent Warburg coefficient and the apparent adsorption resistance, which in equation (7) includes the equilibrium and the rate constants of the chemical reaction:

$$\sigma_{ad}^{ap} \;=\; \sigma_{ad}\,\frac{K_1'}{K_1' + 1} \qquad (8a)$$

And .....

$$R_{ad}^{app} \;=\; R_{ad} + \sigma_{ad}\,\frac{k^{-1/2}}{K_1' + 1} \qquad (8b)$$

On the other hand, in the *high frequency limit*, that applies if $k \ll \omega$, the general adsorption impedance equation (6) is reduced to an expression identical to equation (2), with the same meaning for the frequency independent parameters. Therefore the frequency dependence of the cell impedance obeys equation (3).

We hypothesise that the protonation/deprotonation step is fast, with a rate constant value in the order of the molecular vibrations frequencies ($10^{12}$-$10^{14}$ $s^{-1}$), so in the frequency range used in our measurements the *low frequency limit* of the impedance equation can be applied to the adsorption of adenine from acid solutions, and the adsorption Warburg coefficient values obtained from the analysis of the data at pH 1 must be considered "apparent σ values", because apart from the true Warburg coefficient defined in equation (11) it includes the equilibrium constant of the chemical step, according to equation (8).

**Discussion**

The four frequency independent parameters in eq. (4) include in their definition the kinetic and thermodynamic information of the adsorption process, as expressed in the equations (9-12):

$$C_{dl,\Gamma} = \left( \partial \sigma^M / \partial E \right)_{\Gamma} \tag{9}$$

$$R_{ad} = \left( \partial \sigma^M / \partial \Gamma \right)_E^{-1} \left( \partial v / \partial \mathrm{E} \right)_{\mathrm{c},\Gamma}^{-1} \tag{10}$$

$$\sigma_{ad} = \frac{1}{D^{\frac{1}{2}}} \left( \partial \sigma^M / \partial \Gamma \right)_E^{-1} \left( \partial v / \partial \mathrm{E} \right)_{\mathrm{c},\Gamma}^{-1} \left( \partial v / \partial c \right)_{\mathrm{E},\Gamma} = $$

$$= -\frac{1}{D^{1/2}} \left( \partial \sigma^M / \partial \Gamma \right)_E^{-1} \left( \partial \Gamma / \partial \mathrm{E} \right)_{\mathrm{c}}^{-1} \left( \partial \Gamma / \partial c \right)_{\mathrm{E}} \tag{11}$$

$$C_{ad} = -\left( \partial \sigma^M / \partial \Gamma \right)_E \left( \partial v / \partial \mathrm{E} \right)_{\mathrm{c},\ \Gamma} \left( \partial v / \partial \Gamma \right)_{c,E}^{-1} = \tag{12}$$

$$= -\left(\partial\, \sigma^{M} /_{\partial\, \Gamma}\right)_{E} \left(\partial\, \Gamma /_{\partial\, \mathrm{E}}\right)_{\mathrm{c}}$$

Where $\sigma^{M}$ is the charge density on the metal surface and $D$ is the diffusion coefficient of the adsorbate, which it is assumed to be the same for the two diffusing species in the case of the preceding chemical step.

The values of the four frequency independent parameters obtained from the frequency analysis at every potential along the adsorption wave ( $R_{ad}$, $\sigma_{ad}$ $or$ $\sigma_{ad}^{ap}$, $C_{ad}$ and $C_{dl,\Gamma}$) are plotted as a function of potential in figures 6a-6c. It can be observed that $R_{ad}$ and $\sigma_{ad}$ have a minimum, and $C_{ad}$ exhibits a maximum at potentials around the onset of adenine adsorption.

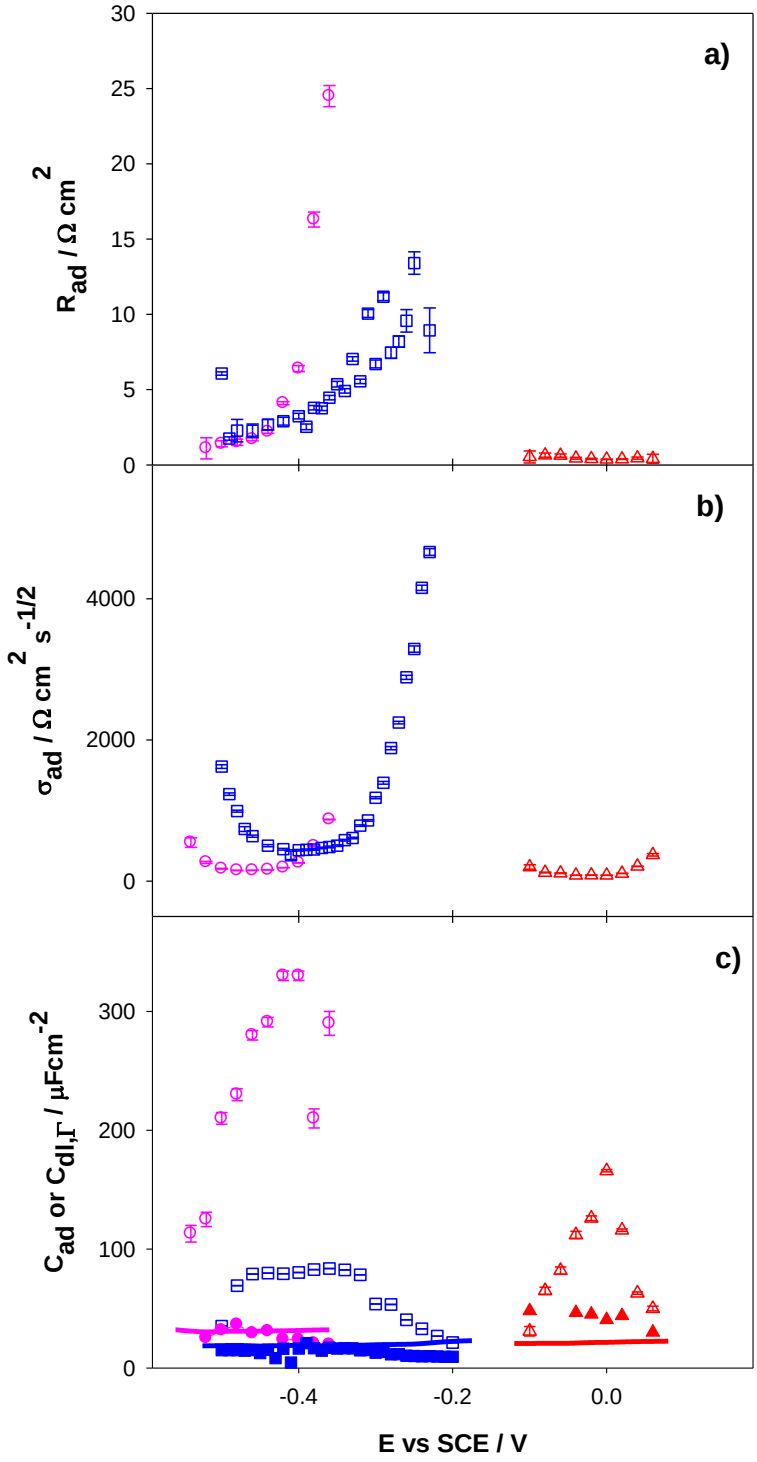


Figure 6.- Plots of $R_{ad} vs\ E$ (a), $\sigma_{ad} vs\ E$ (b) and $C_{ad}$(hollow symbols) and $C_{dl}$(filled symbols) $vs\ E$ (c) obtained from the analysis with the frequency according to equation (4) for the adsorption of adenine on Au(111) from 1mM solutions at pH 1 (triangles), pH 7.5 (squares) and pH 12 (circles). In plot c) the pseudo-capacitance obtained for the supporting electrolyte is included (lines) for comparison. In fig 6b, the values plotted at pH 1 correspond to $\sigma_{ad}^{ap}$. The error bars have been estimated from the standard deviations obtained from fitting procedure.

The $C_{dl,\Gamma}\ vs\ E$ plots in neutral and basic media are nearly coincident with those of the supporting electrolyte in the same conditions at the lower potentials of the adsorption capacitance peaks, and become slightly lower at higher potentials. In acid media the differences with the values in the absence of adenine is somewhat higher, but not significant in view of the lower precision of the frequency analysis (the frequency dispersion of the impedance data is lower) so the $C_{dl,\Gamma}$ values calculated can be considered to be close to the pseudo-capacitance of the supporting electrolyte.

The comparison of $R_{ad},\ \sigma_{ad}$ and $C_{ad}\ vs\ E$ plots obtained at pH 12 and at pH 7.5 shows that at pH 12 the plots are slightly shifted towards lower potentials, about 60 mV for 4.5 pH units. This potential shift with the pH could in principle be ascribed to a different nature of the adsorbate species at each pH values, being the predominant forms of adenine in the bulk solutions the adsorbed species at each of both pHs values, the neutral form at pH 7.5 and the anionic deprotonated form at pH 12. Similar minimum values of $R_{ad}$ are obtained for the adsorption at both conditions, suggesting similar kinetic contributions. On the contrary, significant differences at pH 7.5 and 12 can be observed in the minimum values of $\sigma_{ad}$ and maximum values of $C_{ad}$. At pH 12 these values of $\sigma_{ad}$ and $C_{ad}$ are lower and higher, respectively than the corresponding values at pH 7.5.According to their definitions in equations (11) and (12), both parameters include the partial derivatives $\left(\partial\ \sigma^{M}/_{\partial\ \Gamma}\right)_{E}$ and $\left(\partial\ \Gamma/_{\partial\ \mathrm{E}}\right)_{\mathrm{c}}$ or their inverses in the case of $\sigma_{ad}$. Both factors can be expected to depend on the nature of the adsorbate molecule, especially if the differences between adsorbates at pH 12 and 7.5 involve or not a negative net charge on the molecule. Therefore these differences in the parameters obtained at pH 12 and pH 7.5 are in agreement with the previous spectro-

electrochemical studies [13] that suggested that adsorbed species at pHs 7.5 and 12 are the neutral adenine and the anionic deprotonated adenine, respectively.

Regarding the data at pH 1, the plots of $R_{ad}$, $\sigma_{ad}$ and $C_{ad}$ $vs$ $E$ are shifted c.a. 350 mV towards higher potentials as compared with the plots at pH 7.5. This shift is in agreement with an adsorption process that involves a deprotonation of the predominant cationic species, $AdH_4^+$ in solution. On the other hand, the values of $R_{ad}^{app}$ and $\sigma_{ad}^{ap}$ obtained at pH 1 are lower than those of $R_{ad}$ and $\sigma_{ad}$ at pH 7.5.

Considering that at both pHs the adsorbed species are the neutral form (as shown by the IRRAS experiments [12]) it can be expected that the adsorption/desorption thermodynamic parameters should be equivalent. Then the minimum values of the true Warburg coefficient defined in equation (11) can be considered the same at both pH values. Therefore, from the minimum values of $\sigma_{ad}^{ap}$ and $\sigma_{ad}$ obtained at pH 1 and 7.5, respectively, it is possible to estimate the value of the apparent equilibrium constant $K_1'$ using equation (8a). A value of 0.3±0.1 is obtained in this estimation for $K_1'$ at pH 1, which corresponds to a dissociation constant of the protonated adenine at the interphase of 0.03±0.01. This value of equilibrium constant cannot explain, however, the lower values for $R_{ad}^{app}$ obtained at pH 1 as compared to the $R_{ad}$ values obtained at pH 7.5, because according to equation (8b) and the high value of the rate constant for the deprotonation / protonation reactions the adsorption resistance values obtained at pH 1 must be the true adsorption resistances and should coincide with the values obtained at pH 7.5. The differences will be discussed bellow based on the potential dependence of the rate of adsorption and the shifting of the adsorption potential due to the deprotonation step.

The value for the apparent dissociation constant in the electrode/electrolyte interface is three orders of magnitude higher than the dissociation constant of $AdH_4^+$ in bulk aqueous solutions. The study of the orientation of adsorbed adenine on Au(111) electrode by a quantitative FT-IRRAS method [16] concluded that the neutral adenine form is adsorbed with nitrogen N10 from the amine group and nitrogen N1 from the pirimidinic ring directed towards the electrode. Thus, the interaction of the electric field at the electrode vicinity over the molecular fragment involved in the dissociation equilibrium, N1 and with the protons can be high enough as to explain the value obtained for the dissociation constant of $AdH_4^+$ at the vicinity of the electrode surface. Delgado et al. [17] showed that the second $pK_a$ value of dicarboxylic acids adsorbed on gold electrodes decreases from the bulk solution value as the uncoordinated carboxylic group becomes closer to the electrode surface, and this behaviour is explained as a consequence of the electrostatic interaction of the acid moiety and the positively charged electrode surface.

The combination of the parameters $R_{ad}$, $\sigma_{ad}$ and $C_{ad}$ provides the values of the relaxation times of diffusion, $\tau_D$ , and of adsorption, $\tau_H$ [15].

$$\tau_D^{1/2} = -\frac{\left(\partial\,\Gamma/\partial\,c\right)_{\mathrm{E}}}{(2\,D)^{1/2}} = 2^{-1/2}\sigma_{ad}C_{ad} \qquad (13a)$$

$$\tau_H = \left(\partial\,\Gamma/\partial\,v\right)_{E,c} = R_{ad}C_{ad} \qquad (13b)$$

The estimated values of $\tau_D$ and $\tau_H$ at different potentials are summarised in Table I for the respective adenine adsorptions at the three pH values.

| **pH 1** | **pH 7.5** | **pH12** |
|---|---|---|

| E / V | $\tau_D$/ms | $\tau_H$/ms | E / V | $\tau_D$/ms | $\tau_H$/ms | E / V | $\tau_D$/ms | $\tau_H$/ms |
|---|---|---|---|---|---|---|---|---|
| 0.06 | 3.4 | 2.7 | -0.24 | 18.9 | | -0.36 | 5.9 | 2.7 |
| 0.02 | 1.3 | 1.0 | -0.26 | 13.7 | 0.4 | -0.38 | 6.3 | 2.9 |
| 0.00 | 1.6 | 1.3 | -0.28 | 10.2 | 0.4 | -0.40 | 2.8 | 1.6 |
| -0.02 | 1.3 | 1.0 | -0.30 | 4.0 | 0.4 | -0.42 | 2.8 | 1.3 |
| -0.04 | 1.1 | 0.9 | -0.32 | 3.8 | 0.4 | -0.44 | 0.7 | 0.6 |
| -0.06 | | | -0.34 | 2.3 | 0.4 | -0.46 | 0.7 | 0.5 |
| -0.08 | 5.3 | | -0.36 | 1.6 | 0.4 | -0.48 | 0.3 | 0.4 |
| -0.10 | 0.9 | 0.7 | -0.38 | 1.4 | 0.3 | -0.50 | 0.4 | 0.4 |
| | | | -0.40 | 1.2 | 0.3 | -0.52 | 0.3 | 0.3 |
| | | | -0.42 | 1.3 | 0.2 | -0.54 | 0.1 | 0.1 |
| | | | -0.44 | 1.6 | 0.2 | | | |

**Table I.**- Values of the relaxation times in milliseconds of diffusion and of adsorption obtained according to equations (13) for the adsorption of adenine on Au(111) electrodes from 1 mM solutions at the indicated pH values.$\tau_D$ at pH 1 have been calculated correcting the apparent Warburg coefficient according to equation (8)

In can be observed that both relaxation times are of the same order of magnitude (data at pH 1 and at pH 12) or are about one order of magnitude higher for $\tau_D$ (in the case of the data at pH 7.5). This confirms the mixed kinetic control of the process by diffusion and by adsorption activation in the case of the adsorption at pH 1 and 12 and the control mostly by diffusion in the case of the adsorption at pH 7.5, that was inferred from the Nyquist plots of the electrode admittance in figure 4.

A more quantitative picture of the adsorption kinetics can be obtained from the values of the specific rate of adsorption, $k_{ad}f_{ad}(\Gamma)$, that can be obtained from $R_{ad}$ and $\sigma_{ad}$ according to equations (10) and (11):

$$k_{ad}f_{ad}(\Gamma) = D^{1/2}\frac{\sigma_{ad}}{R_{ad}} \qquad (14)$$

The plots of $k_{ad} f_{ad}(\Gamma)$ as a function of the potential are shown in figure 7 at the three investigated pH conditions.

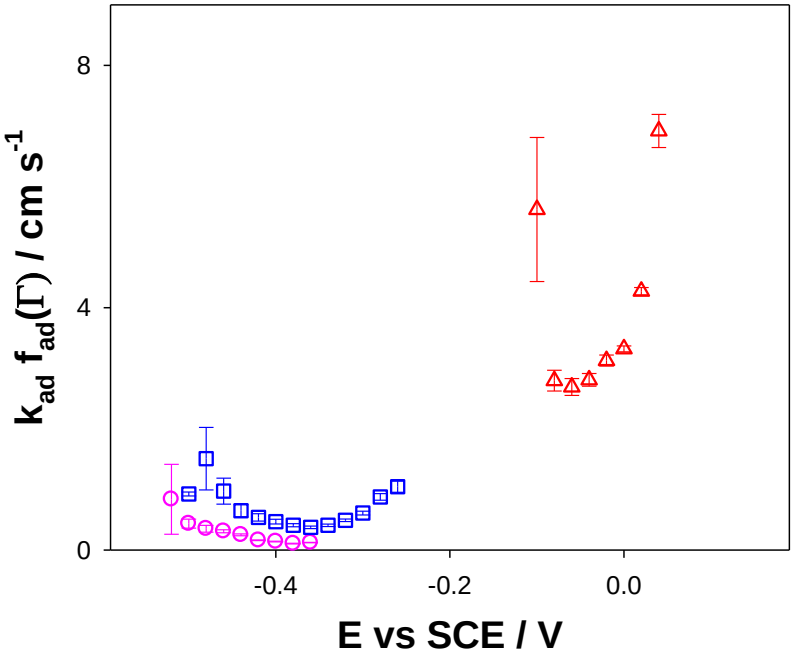


Figure 7.- $k_{ad}\ f_{ad}(\Gamma)\ vs\ E$ plots calculated with the parameters obtained from the analysis with the frequency and equation (14) at pH 1 (triangles), pH 7.5 (squares) and pH 12 (circles). The $\sigma_{ad}^{app}$ values obtained at pH 1 have been corrected according to equation (8a).

At pH 7.5 two different behaviours of the specific rate constant can be distinguished with the potential. At low potentials $k_{ad}\ f_{ad}(\Gamma)$ decreases with the potential, it reaches a minimum value and then increases with the potential. At pH 12 the available potential range is shorter and only the first tendency is obtained. At pH 1, the specific rate constant obtained is higher than at pH 7.5, and an increasing tendency with potential can be inferred.

Opposite contributions to the potential behaviour can be expected for $k_{ad}$ and for $f_{ad}(\Gamma)$. For $k_{ad}$ a Butler Volmer type dependence with the potential was proposed by Szulborska and Baranski [18,19], while $f_{ad}(\Gamma)$ is a monotonic decreasing function of the surface excess with an explicit expression that depends on the adsorption isotherm

that applies to the system. The simplest form of $f_{ad}(\Gamma)$ corresponds to a Langmuir's isotherm, for which the expression (15) holds:

$$f_{ad}(\Gamma) = \frac{k_{ad}\, c}{k_{ad}\, c \;\; + \; k_d} \quad \text{(Langmuir's isotherm)} \qquad (15)$$

Equation (15) introduced in the definition of the specific rate of adsorption yields a similar behaviour with the potential, increasing or decreasing, for both $k_{ad} f_{ad}(\Gamma)$ and $k_{ad}$. However, an increasing behaviour with the potential can be expected for $k_{ad}$ and the opposite is clearly found for $k_{ad} f_{ad}(\Gamma)$ at pH 12 and at low potentials at pH 7.5. Therefore, the kinetic results cannot be explained with a Langmuir's isotherm for the adsorption of adenine.

The thermodynamic study of adenine adsorption in neutral media concluded that the adsorption obeys a Frumkin isotherm, with an attractive interaction parameter [2]. Therefore, the lateral interactions between the adsorbate molecule in the transition state of the adsorption step and in the final ground state must be taken into account in the kinetic expression, as suggested by Szulborska and Baranski [19] for the adsorption of thioglycol on mercury electrodes.

$$f_{ad}(\Gamma) = \frac{\Gamma_{max} - \Gamma}{\Gamma_{max}} \exp\left(\frac{2\, g^{\neq}\, \theta}{RT}\right) \quad \text{(Frumkin's isotherm)} \qquad (16)$$

Where $g^{\neq}$ is the interaction parameter between the activated complex of the adsorption step and the adsorbate in its ground state and $\theta = {}^{\Gamma}/_{\Gamma_{max}}$ is the surface coverage. $g^{\neq}$ affects both energy barriers of the adsorption and desorption steps, and must be related to the thermodynamic interaction parameter, $g$:

$$\frac{g^{\neq}}{g} = \frac{\left(\partial \Delta G_{ads}^{\neq} / \partial \theta\right)_E}{\left(\partial \Delta G_{ads}^{0} / \partial \theta\right)_E} = \left(\frac{\partial \Delta G_{ads}^{\neq}}{\partial \Delta G_{ads}^{0}}\right)_{\mathrm{E}} \qquad (17)$$

From equation (17) it is inferred that the ratio $g^{\neq}/g$ is some type of symmetry factor and it could be considered like a charge transfer coefficient in an electron transfer, so its value must be between 0 and 1.

A $g^{\neq}/g$ value close to 1 provided an explanation to the potential dependence of the specific rate constant of the adsorption of adenine on Au(111) from neutral pH solutions [4], assuming a Butler-Volmer type dependence of $k_{ad}$ with the potential.

At higher potentials, if the bulk concentration of the adsorbate is lower than the required value to saturate the surface, according to equation (16) the function $f_{ad}(\Gamma)$ must reach a minimum value. From the potential of $f_{ad}(\Gamma)$ minimum all the potential dependence of the specific rate constant obeys to the dependence of $k_{ad}$, explaining the exponential increase of $k_{ad}f_{ad}(\Gamma)$ with the potential at high potentials observed at pH 7.5 in figure 7.

For the adsorption of adenine from basic solutions, taking into account that the adsorbate is the anionic species $AdH_2^-$, the electrostatic interactions between the transition state of adsorption and the adsorbate molecules in their ground state must originate a lower interaction parameter than in neutral media. According to equation (16) this would explain the lower specific rate obtained at pH 12.

On the other hand, the higher values of the specific rate constant obtained at pH 1 as compared to the values at pH 7.5 can also be explained by the dependence of $k_{ad}$ with

the potential. The shift in the adsorption/desorption equilibrium potentials caused by the deprotonation step originates also the shifting of the adsorption potential towards higher values at which the rate constant for the adsorption step, $k_{ad}$ is in the exponentially increasing with potential region.

## CONCLUSIONS

The dispersion with the frequency obtained for the pseudocapacitance data of adenine adsorption on Au(111) electrodes can be explained on the basis of an adsorption kinetic model according to the work of Frumkin and Melik-Gaikazayan. This model does not involve any assumption about the type of isotherm that applies or about the potential dependence of the adsorption rate constant. In the adsorption of adenine from very acid solutions a deprotonation step preceding the adsorption step has been considered in the kinetic model. The general impedance equations corresponding to this model can be simplified to the *low frequency* limiting case which is applicable when the rate constant of the chemical step is high as compared to the experimental frequency values, yielding the same frequency dependence of the impedance data than the original model (which does not include the chemical step) but with a different meaning for the apparent adsorption Warburg coefficient and adsorption resistance.

The analysis of the real and imaginary components of the electrode admittance has provided the values of the adsorption parameters $R_{ad}$, $\sigma_{ad}$ and $C_{ad}$ as a function of the potential. From the $\sigma_{ad}$ vs E plot obtained at pH 1 an equilibrium constant for adenine deprotonation three orders of magnitude higher than the equilibrium constant in the bulk solution has been calculated. The frequency independent parameters allow us to calculate the relaxation times of adsorption and diffusion, and the specific rate of the adsorption process. From the relaxation times a mixed kinetic control by diffusion and

by adsorption activation is inferred for the adsorption from solutions of pH 1 and 12, but a somewhat higher kinetic control by diffusion in the case of the adsorption from solutions of pH 7.5. The potential dependence of the specific adsorption rate is explained as the result of the combined potential dependence of a Frumkin type $f_{ad}(\Gamma)$ function with an attractive interaction parameter and a Butler-Volmer potential dependence type for $k_{ad}$. This potential dependence justifies the higher values obtained for $k_{ad}f_{ad}(\Gamma)$ at pH 1 as compared to the values obtained at pH 7.5, as the equilibrium of the preceding chemical step shifts the adsorption process to higher potentials. The lower values obtained for $k_{ad}f_{ad}(\Gamma)$ at pH 12 suggest a lower value for the interaction parameter of the corresponding Frumkin isotherm for the adsorption of anionic adenine as compared to neutral adenine form.

## ACKNOWLEDGEMENTS

Financial support from the Spanish Ministry of Economy and Competitiveness (CTQ2014-57515-C2-1-R and ELECTROBIONET- CTQ2015-71955-REDT) and from the Junta de Andalucia (PAI FQM202) is gratefully acknowledged. JAM acknowledges a FPU grant from the Spanish Ministry of Science and Technology.

## REFERENCES

[1] J. Clavilier, R. Faure, G. Guinet, R. Durand, Preparation of monocrystalline Pt microelectrodes and electrochemical study of the plane surfaces cut in the direction of the {111} and {110} planes, J. Electroanal. Chem. Interfacial

Electrochem. 107 (1980) 205–209. doi:10.1016/S0022-0728(79)80022-4.

[2] C. Prado, F. Prieto, M. Rueda, J. Feliu, A. Aldaz, Adenine adsorption on Au(111) and Au(100) electrodes: Characterisation, surface reconstruction effects and thermodynamic study, Electrochim. Acta. 52 (2007) 3168–3180. doi:10.1016/j.electacta.2006.09.062.

[3] C. Vaz-Domínguez, M. Escudero-Escribano, A. Cuesta, F. Prieto-Dapena, C. Cerrillos, M. Rueda, Electrochemical STM study of the adsorption of adenine on Au(111) electrodes, Electrochem. Commun. 35 (2013) 61–64. doi:10.1016/j.elecom.2013.07.045.

[4] F. Prieto, M. Rueda, C. Prado, J.M. Feliu, A. Aldaz, Kinetics of adenine adsorption on Au(1 1 1) electrodes: An impedance study, Electrochim. Acta. 55 (2010) 3301–3306. doi:10.1016/j.electacta.2009.12.105.

[5] A. Frumkin, V. Melik-Gaykazyan, Determination of the Kinetics of Adsorption of Organic Substances by a.-c. Measurements of the Capacity and the Conductivity at the Boundary: Electrode-Solution, Dokl. Acad. Nauk. 77 (1951) 855–858.

[6] T. Pajkossy, T. Wandlowski, D.M. Kolb, Impedance aspects of anion adsorption on gold single crystal electrodes, J. Electroanal. Chem. 414 (1996) 209–220. doi:10.1016/0022-0728(96)04700-6.

[7] T. Pajkossy, Capacitance dispersion on solid electrodes: anion adsorption studies on gold single crystal electrodes, Solid State Ionics. 94 (1997) 123–129. doi:10.1016/S0167-2738(96)00507-3.

[8] Z. Kerner, T. Pajkossy, Measurement of adsorption rates of anions on Au(111)

electrodes by impedance spectroscopy, Electrochim. Acta. 47 (2002) 2055–2063. doi:10.1016/S0013-4686(02)00073-7.

[9] D. Eberhardt, E. Santos, W. Schmickler, Impedance studies of reconstructed and non-reconstructed gold single crystal surfaces, J. Electroanal. Chem. 419 (1996) 23–31. doi:10.1016/S0022-0728(96)04872-3.

[10] J.M. Broomhead, The Structures of Pyrimidines and Purines. II. A Determination of the Structure of Adenine Hydrochloride by X-ray Methods, Acta Crystallogr. 1 (1948) 324–329.

[11] J.M. Broomhead, The structures of pyrimidines and purines. IV. The crystal structure of guanine hydrochloride and its relation to that of adenine hydrochloride, Acta Crystallogr. 4 (1951) 92–100. doi:10.1107/S0365110X51000349.

[12] M. Rueda, F. Prieto, A. Rodes, J.M. Delgado, In situ infrared study of adenine adsorption on gold electrodes in acid media, Electrochim. Acta. 82 (2012) 534–542. doi:10.1016/j.electacta.2012.03.070.

[13] J. Álvarez-Malmagro, F. Prieto, M. Rueda, A. Rodes, In situ Fourier transform infrared reflection absorption spectroscopy study of adenine adsorption on gold electrodes in basic media, Electrochim. Acta. 140 (2014) 476–481. doi:10.1016/j.electacta.2014.03.074.

[14] F. Prieto, M. Rueda, J. Álvarez-Malmagro, Electrochecmical Impedance Spectroscopy analysis of an adsorption process with coupled preceding chemical step., Electrochim. Acta. In press (2017). doi:http://dx.doi.org/10.1016/j.electacta.2017.02.106.

[15] M. Sluyters_Rehbach, Impedance of electrochecmical systems: Terminology, nomenclature and representation. Part I: Cells with metal electrodes and liquid solutions, Pure Appl. Chem. 66 (1994) 1831–1891.

[16] F. Prieto, Z. Su, J.J. Leitch, M. Rueda, J. Lipkowski, Quantitative Subtractively Normalized Interfacial Fourier Transform Infrared Reflection Spectroscopy Study of the Adsorption of Adenine on Au(111) Electrodes, Langmuir. 32 (2016) 3827–3835. doi:10.1021/acs.langmuir.6b00635.

[17] J.M. Delgado, A. Berná, J.M. Orts, A. Rodes, J.M. Feliu, In Situ Infrared Study of the Adsorption and Surface Acid−Base Properties of the Anions of Dicarboxylic Acids at Gold Single Crystal and Thin-Film Electrodes, J. Phys. Chem. C. 111 (2007) 9943–9952. doi:10.1021/JP071489M.

[18] A. Szulborska, A. Baranski, Numerical simulation of kinetically controlled electrosorption processes under cyclic voltammetric conditions, J. Electroanal. Chem. 377 (1994) 23–31. doi:10.1016/0022-0728(94)03437-0.

[19] A. Szulborska, A. Baranski, Kinetics and thermodynamics of thioglycol adsorption on mercury ultramicroelectrodes, J. Electroanal. Chem. 377 (1994) 269–281. doi:10.1016/0022-0728(94)03438-9.